

# On the Origin of Slow and Large Earthquakes in South-Central Mexico

Víctor M. Cruz-Atienza<sup>a\*</sup>, Carlos Villafuerte<sup>a</sup>, Vladimir Kostoglodov<sup>a</sup>, Josué Tago<sup>b</sup>,  
Raymundo Plata-Martínez<sup>a</sup>, Sara Franco<sup>a</sup>, Ekaterina Kazachkina<sup>a</sup> and Jorge Real<sup>a</sup>

<sup>1</sup>Instituto de Geofísica, Universidad Nacional Autónoma de México

<sup>2</sup>Facultad de Ingeniería, Universidad Nacional Autónoma de México

\*Corresponding author: [cruz@igeofisica.unam.mx](mailto:cruz@igeofisica.unam.mx)

This manuscript has not been peer-reviewed and  
was submitted to EPSL in August 2025

## Abstract

Slow slip events (SSEs) in Guerrero and Oaxaca, Mexico, have likely triggered five of the last six M7+ earthquakes in the region since 2012. This interaction, however, is non-systematic, as evidenced by the preceding 17 years of large earthquake quiescence, when multiple SSEs occurred without consequence. The Mexican catalog since 1800 reveals that large earthquakes cluster in time every ~15 years, suggesting that the subduction zone periodically reaches a critical state where SSEs become seismic precursors. The regional inter-SSE coupling pattern is highly consistent with the SSEs bimodal spatial distribution, with the maximum associated stresses being released by successive SSEs at depths of 25 to 40 km. In the eastern and western bordering regions where SSEs are negligible, the coupling becomes shallower and encompasses the historical rupture areas. The occurrence of tectonic tremor, low-frequency and repeating earthquakes, together with the friction condition of the plate interface, indicate (1) a major velocity weakening zone where long-term SSEs develop; and (2) two limiting zones of transition to free-slip where velocity strengthening friction becomes critically stressed, seismic radiation is maximum, and slip is intermittent producing short-term SSEs. The offshore segment of the Guerrero seismic gap where shallow SSEs were recently discovered is the most frictionally stable region, a condition that partly explains the absence of large earthquakes since 1911. The long-term slip deficit rate at the plate interface is found to be consistent (within 14% error) with sequences of large (M7+) repeating earthquakes throughout the region.

## 1. Introduction

Slow slip events (SSE) in Mexico have been widely studied in the last two decades (Brudzinski et al., 2007; Cavalié et al., 2013; Correa-Mora et al., 2009, 2008; Cruz-Atienza et al., 2021; Cruz-Atienza et al., 2025; Franco et al., 2005; Graham et al., 2016, 2014; Iglesias et al., 2004; Kostoglodov et al., 2010, 2003; Lowry et al., 2001; Radiguet et al., 2012, 2011; Vergnolle et al., 2010; Villafuerte et al., 2025; Walpersdorf et al., 2011). Their distinction and segmentation along the Middle America Trench between the states of Guerrero and Oaxaca are attributed to the subhorizontal geometry of the plate interface in Guerrero, which makes conductive depths for SSEs more extensive, and the subduction of fracture zones in the Cocos oceanic plate (Cruz-Atienza et al., 2025a).

Seismicity is a fundamental indicator of tectonic activity. Tectonic tremor (TT) and low-frequency earthquakes (LFE) are particularly sensitive to slow dislocations at the plate contact, as demonstrated by the strong link between SSE and the sources of these seismic signals in several subduction zones worldwide (Frank et al., 2015; Obara et al., 2004; Rogers and Dragert, 2003). In south-central Mexico, the spatio-temporal correlation between them has gradually been uncovered and understood (Brudzinski et al., 2010; Cruz-Atienza et al., 2015; Frank et al., 2013; A.L. Husker et al., 2012; Kostoglodov et al., 2010; Maury et al., 2016; Payero et al., 2008). It is now clear that the most common TTs and LFEs in Guerrero occur at depths close to the plate interface, i.e. between ~35 and ~45 km depth, where dense instrumentation has allowed this to be established (Frank et al., 2014; Villafuerte and Cruz-Atienza, 2017).

Despite their modest manifestation, smaller and more frequent SSEs have also been identified in the deep segment of the plate interface (i.e., short-term SSEs) (El Yousfi et al., 2023; Frank et al., 2015; Kostoglodov et al., 2010; Rousset et al., 2017; Villafuerte and Cruz-Atienza, 2017), where most of TTs and LFEs occur featuring rapid migrations associated with non-linear fluid diffusion in the subduction channel (Cruz-Atienza et al., 2018b; Frank et al., 2014). Intermittence of slow slip has also been proposed to explain successive tremor bursts and clustering (El Yousfi et al., 2023; Frank et al., 2018). The source mechanism of the tremor corresponds to shallow thrust dislocations, consistent with plate geometry and convergence direction, as revealed by collocated very-low-frequency earthquakes (VLFE) (Maury et al., 2018, 2016). In the shallow segment of the interface (i.e. above ~20 km), repeating earthquakes are the most common and easily detectable expression of aseismic slip in both states (Dominguez et al., 2016), suggesting the episodic slow activation of the interface mostly offshore (Dominguez et al., 2022; Plata-Martinez et al., 2021). Detections of TTs and LFEs offshore Guerrero using ocean bottom seismometers confirms this (Chen et al., 2025; Cruz-Atienza et al., 2018a; Plata-Martinez et al., 2021), where the first two shallow SSEs in Mexico were recently discovered using seafloor geodesy (Cruz-Atienza et al., 2025b).

## Figure 1

This paper summarizes the current knowledge on slow earthquakes in south-central Mexico and analyses their role in the seismic cycle in order to identify the dominant seismogenic features of the region. To this end, we examine the historical SSE catalog introduced by Cruz-Atienza et al. (2025a) (Figure 1), together with the long-term inter-SSE deformation periods, using new and consistent GPS data processing and inversion techniques. This analysis, combined with all the available information on slow and repeating earthquakes, provide a comprehensive picture of the mechanical stability and the processes occurring at the plate interface, and their relationship to large subduction earthquakes.

## 2. Results

### 2.1. Slow slip and seismic radiation

Cruz-Atienza et al. (2025a) introduced a comprehensive catalog of SSEs in the Mexican subduction zone since 1997. From this catalog, Figure 1 illustrates the along-trench extent and timing of all known SSEs in the states of Guerrero and Oaxaca, together with the most recent M7+ earthquakes in the region. As illustrated, it is clear that prior to the onset of the

earthquake cluster in 2012, there was a prolonged period of quiescence spanning 17 years from the Copala earthquake in 1995 (Couboulex et al., 1997). The average slip distribution of the SSEs from the catalog is shown in Figure 2 (blue shades with contours indicating the 15%, 40% and 80% iso-slip values), together with the earthquakes epicenters and the historical rupture areas. SSEs over multiple cycles clearly delineate a cumulative slow slip segmentation along the Middle America Trench, with two maxima: one in Guerrero to the west, with the largest slip values, and the other in Oaxaca to the east. Both cumulative maxima occur at depths between 30 and 40 km.

### Figure 2

When comparing the SSEs slip distribution with the associated seismicity reported in the literature (Figure 2) (Brudzinski et al., 2010; Chen et al., 2025; Dominguez et al., 2022; El Yousfi et al., 2023; Frank et al., 2014; Maury et al., 2018; Plata-Martinez et al., 2021; Rousset et al., 2017; Villafuerte and Cruz-Atienza, 2017), the most striking observation is the absence of tremor, LFEs and repeaters where the SSEs release the greatest stress between 20 and 40 km depth. This observation aligns with previous findings in the Nankai subduction zone (Nishikawa et al., 2023; Obara and Kato, 2016) and suggests that the seismic radiation associated with slow slip predominantly occurs along the transition to free slip of the megathrust (above ~20 km and below ~40 km). The observed clustering and intermittence of LFEs, together with their associated slip (El Yousfi et al., 2023; Frank et al., 2018; Jolivet and Frank, 2020), reflect activity confined to relatively narrow zones of the plate boundary flanking broader regions of dominant slow energy release. Therefore, it is not yet clear whether SSEs behave consistently (i.e. intermittently in the short term) along the extensive interface regions where they are preponderant.

### Figure 3

The short-term SSEs in Guerrero (Frank et al., 2015; Rousset et al., 2017; Villafuerte and Cruz-Atienza, 2017) appear to be confined to the area where slow and repeating earthquakes are generated and where less than 40% of the long-term transient slip occurs (green shades, Figure 2). This suggests that the zones surrounding the large slip regions are primarily those susceptible to intermittence of slow slip. Figures 3 and 4 show two cross sections where this is clear. In the case of Guerrero (Figure 3), slow and repeating earthquakes occur where long-term SSEs fade out and short-term events occur. Of particular interest is the overlap of both types of SSEs at seismogenic depths in this region. This observation, which differs from Oaxaca (Figure 4), suggests a reasonable, at least partial explanation for the absence of large earthquakes within the Guerrero seismic gap, where the slow and recurrent release of elastic strain energy delays potentially devastating seismic events (Cruz-Atienza et al., 2025b). In the case of Oaxaca, although the hypocentral uncertainty of tremor is greater, the along-dip segmentation of seismic radiation is also evident (Figure 4c). As observed in Guerrero, tremor occurrence coincides with the presence of short-term SSEs at the deep part of the plate interface (El Yousfi et al., 2023), where long-term SSEs fade out. At shallow depths above 25 km, although no tremor is observed yet, repeaters indicate aseismic slip up-dip from the coupled seismogenic segment, next to the trench (Dominguez et al., 2022). Overall results, which are consistent in both Guerrero and Oaxaca, indicate a segmentation of the interface mechanical properties along the dip, with slip tending to increase its intermittency while radiating seismic energy as we approach free-slip depths.

Figure 4

## 2.2. Dynamic stability of the plate contact

Only the inter-SSE periods are predominantly stable during the seismic cycle. In these earthquake- and SSE-free periods, the plate interface remains coupled to some degree and transfers deformation to the continental plate approximately in a stationary manner. The mechanical condition of the plate interface during these periods is particularly important for the dynamic stability of the megathrust because slip instabilities (either slow or fast) arise from this condition. Under such quasi-steady inter-SSE state, the interface slip velocity,  $v$ , is approximately constant and generally less than plate convergence rate (i.e. coupling regime). The shear strength of the plate contact at steady state,  $\tau_{ss}$ , depends on this velocity and the effective normal stress,  $\sigma_{ss}$ , such that

$$\tau_{ss} = f' \sigma_{ss} + (a - b) \sigma_{ss} \ln \left( \frac{v}{v_{pl}} \right), \quad (1)$$

where  $a$  and  $b$  are friction constitutive parameters and the constant  $f'$  is the steady state friction coefficient at plate convergence velocity  $v_{pl}$  (Dieterich, 1979; Ruina, 1983). Thus, the Coulomb failure stress,  $CFS = \tau_{ss} - f' \sigma_{ss}$ , derived with respect to  $\ln(v)$ , reads (Hsu et al., 2006; Weiss et al., 2019)

$$d(CFS)/d(\ln(v)) = (a - b) \sigma_{ss}. \quad (2)$$

This remarkable result provides a useful framework to determine the regions that contribute to the dynamic stability or instability of the plate interface from the observed inter-SSE strain rate. This is because depending on the sign of  $(a - b)$ , friction is either velocity strengthening (VS) and therefore stable (or conditionally stable) where  $(a - b) > 0$ , or velocity weakening (VW) and therefore unstable where  $(a - b) < 0$  (Scholz, 2018). In general,  $\sigma_{ss}$  increases with depth or remains relatively constant where overpressured fluids are present at the interface (e.g., Liu and Rice, 2005). Therefore, changes in the sign of  $(a - b) \sigma_{ss}$  are representative of overall variations in the frictional stability regime.

To estimate the inter-SSE deformation pattern and thus the associated plate interface coupling (PIC), we first examined the available historical GPS records in Guerrero and Oaxaca to identify well-defined steady inter-SSE periods. The data is sourced from the GPS networks operated by the Mexican Seismological Service (SSN), the Department of Seismology of the Institute of Geophysics of UNAM and Tlalocnet (Cabral-Cano et al., 2018). Following Villafuerte et al. (2025) and Cruz-Atienza et al. (2025b), seasonal noise reduction was applied to all GPS time series. We defined the strain rate at each station as the average of the displacement rates estimated by linear regressions of all identified inter-SSE periods. For sites with limited record (less than  $\sim 3$  years, about 10%), only one inter-SSE period was considered. In Guerrero, the estimates were complemented with those obtained by Cruz-Atienza, et al. (2025b). Representative examples of the linear regressions are shown in Figure S1. A total of 46 sites in both states were carefully selected to determine the deformation velocities shown in Figure S2 (red arrows). The consistency between velocity vectors at nearby stations is remarkable. From these data we determined the PIC distribution in the region, defined as  $1 - v/v_{pl}$ , where



$v$  is the interplate slip rate (Equation 1),  $v_{pl}$  is the average plate convergence rate for the study region (i.e., between longitudes  $-101.5^\circ$  and  $-96^\circ$ ) equal to  $6.8 \pm 0.3$  cm/yr (MORVEL model, DeMets et al., 2010) and  $v \leq v_{pl}$ .

To invert the PIC, we used ELADIN (ELastostatic ADjoint INversion) (Tago et al., 2021), a well-established method for imaging slip at the plate interface from geodetic data with physically consistent constraints such as rake angle, admissible backslip, and spectral content along a three-dimensional geometry of the plate interface (Aguilar-Velázquez et al., 2025; Cruz-Atienza et al., 2025b, 2021; Villafuerte et al., 2025). The plate interface has been discretized with 10 km square subfaults, assuming a geometry that incorporates the most recent seismotectonic information available for both states of Guerrero and Oaxaca (Cruz-Atienza et al., 2021). For the inversion we assumed optimal regularization values for the Hurst exponent of 0.75 and the correlation length of 40 km (Cruz-Atienza et al., 2025b). Mobile checkerboard (MOC) resolution tests with this parameterization are shown in Figures S3 and S4 for 100 km and 70 km slip patches, respectively. The problem solution, the data fit and the 80% restitution index threshold (i.e., the boundary of nominal error less than 20%) for 70 km slip patches, is shown in Figure S2. Note that most of the recovered coupling falls within this limit, including large offshore regions, especially where station coverage is the denser, such as in Guerrero.

### Figure 5

Figure 5 shows a comparison of the mean distribution of SSEs (panel a) with the distribution of inter-SSE coupling (panel b). The most striking observation in this comparison, derived from independent analyses, is the spatial correlation between the slow-slip and coupling maxima within longitudes  $-101^\circ$  and  $-97.5^\circ$ , with a clear segmentation between the two states. Also noteworthy in this longitude range is the relative amplitude between the two coupling maxima, where the greatest maximum (PIC > 0.9) coincides with the largest SSEs in Guerrero. There is also a significant along-strike variation of coupling in the offshore region. For instance, in the Guerrero seismic gap (between longitudes  $-101^\circ$  and  $100^\circ$ ), the coupling is much smaller than in neighboring segments, as found in previous investigations (Cruz-Atienza et al., 2025b; Radiguet et al., 2016; Rousset et al., 2016). Within the seismic gap, the PIC decreases rapidly in the updip direction, reaching values below 0.1 approximately 20 km offshore. The last remarkable observation is at the edges of the study region (i.e., longitudes west of  $-101^\circ$  and east of  $-97.5^\circ$ ), where no significant SSEs occur. In these regions, high PIC values exceeding 0.5 are found offshore and beneath the coast, where large earthquakes have historically and recently occurred, including the 2014 Mw7.4 Papanoa (Guerrero) and 2020 Mw7.2 Huatulco (Oaxaca) events.

Figure 5c shows the distribution of the dynamic condition  $(a - b)\sigma_{ss}$ , determined from the CFS rate, estimated using an artifact-free triangular dislocation model (Nikkhoo and Walter, 2015), and the slip rate at the interface (Equation 2), which are both derived from the inter-SSE coupling distribution (see Supplementary Figure S5). Several prominent features emerge. (1) In regions where the SSEs are maximum (brown contours), the interface is mechanically unstable (i.e. VW), as predicted by rate and state friction SSE models of the region (Cruz-Atienza et al., 2021; Perez-Silva et al., 2021). (2) The most mechanically stable (i.e. VS) region lies offshore of the Guerrero seismic gap. In this region, where the PIC vanishes, the interface is intrinsically stable (i.e. VS) for more than 100 km, where no M7+ earthquakes have occurred

since 1911. (3) At the edges of the study domain beneath the coast (i.e. longitudes west of -101 and east of -97.5), where large earthquakes have occurred in the past, the interface is intrinsically unstable (i.e. VW), particularly in the eastern segments of the 1965, 1978 and 2020  $M \geq 7.3$  earthquakes in Oaxaca (Martínez-López et al., 2025). Figure S6 shows four cross-sections of  $(a - b)\sigma_{ss}$  where the along-strike differentiation of this condition is evident.

### 2.3. Subduction zone stress and slip budget

Since the discovery of SSEs, the scientific community has wondered what role they play in the seismic cycle. It is now clear that the most common phenomenon at the plate interface is these slow instabilities involving a rearrangement of crustal deformations. Numerous studies on SSEs have led to a significant shift in our understanding of the seismic cycle. It is now understood that there is no secular, stationary deformation regime between two large earthquakes as previously thought. In reality, deformation in subduction zones is characterized by slow elastic rebounds caused by SSEs, and by nearly stable deformation periods between them (inter-SSE periods; Figure S1). Within this cycle, and on rare occasions, large earthquakes occur in the subduction system with their elasto-mechanical consequences. The long-term GPS records in Mexico and the comprehensive catalogue of SSEs from Cruz-Atienza et al. (2025a) offer the possibility of making a balance of the long-term crustal deformation to address the question posed above. That is, to better understand which are the processes that contribute most to the seismogenesis of large earthquakes. Specifically, this translates into assessing to what extent is plate coupling and to what extent are the SSEs responsible for these ruptures in the long term.

The long-term strain rate in a subduction zone should indicate the regions most prone to large earthquakes (e.g., Chlieh et al., 2011; Nocquet et al., 2016). However, reliable estimation of such a rate in Mexico is a difficult task due to recurrent SSEs and limited data (Figure S1). An alternative way to estimate the long-term deformation is based on the balance between the deformation induced by coupling during inter-SSE periods and the deformation induced by multiple SSEs cycles. As they are intrinsically part of the same cycle, one expects both deformation patterns to be closely related. That is, the inter-SSE deformation, which represents approximately the steady state prior to slip instabilities, should determine the regions where SSEs occur – because dynamic and/or mechanical transient deviations from that state lead to the instabilities.

### Figure 6

Figure 6a shows the cumulative CFS derived from the inter-SSE coupling distribution shown in Figure 5b over a period of twenty years, which is the timeframe covered by the SSE catalogue in Guerrero (Cruz-Atienza et al., 2025a), from 2002 to 2022 (Figure 1). This estimate is simply obtained by multiplying the inter-SSE stressing rate (Figure S5, top panel) by the number of years in the chosen timeframe. As expected, regions with high coupling experience the highest CFS values, which correlate with the frictionally unstable (VW) segments shown in Figure 5c (i.e., where SSEs and large earthquakes occur regularly). However, since inter-SSE periods are interrupted by SSEs in specific areas over the years, the estimated cumulative CFS (Figure 6a) is overestimated to some extent and should therefore be treated as an upper bound.

In order to estimate the cumulative CFS associated with all SSEs over the same twenty-year period, we need a comprehensive catalogue of the entire study area. However, in Oaxaca, we only have a catalogue from 2017 onwards (i.e., five inverted slow events; Cruz-Atienza et al., 2025a). To approximate the complete history in Oaxaca, we added the average of the inverted SSEs as many times as there were events occurrences in that state between 2002 and 2017 (i.e., nine events, Figure 1). Thus, Figure 6b shows the sum of all CFS distributions associated with the 23 known long-term SSEs in the region. Compared to Figure 6a, while the amplitude of both distributions is similar, there is a clear spatial anti-correlation, as expected. In deep regions (>25 km), the CFS produced by coupling is overall released by successive SSEs. However, in regions below the shoreline where large earthquakes occur regularly, the seismogenic contributions of CFS from both processes vary along the strike. While CFS in regions A and D (compare Figures 6a and 6b) is dominated by the effect of coupling, in region C, contributions from SSEs and coupling are similar. In region B, which corresponds to the Guerrero seismic gap, it is mainly the long-term SSEs that induce offshore seismogenic stresses.

### Figure 7

Figure 7 provides a clearer view of the contributions to the CFS from both processes within two depth ranges. The anticorrelation of the contributions is clear at depth, between 30 and 40 km (panel b), so that the cumulative CFS due to the interplate coupling is roughly balanced by the cumulative CFS from SSEs. This also means, as expected, that the interface segments most loaded by coupling produce the largest slow slips. In contrast, at seismogenic depths of 8–25 km (panel c), along-strike stress heterogeneity primarily originates from the coupling regime, with two maxima at the study domain extremes (segments A and D) and a minimum along the seismic gap (segment B). SSEs, on the other hand, contribute moderately to seismogenesis across segments A, B and C, whereas no significant effect is observed in segment D. Interestingly, in segment C, where a large number of earthquakes have occurred, the contribution of seismogenic stress from coupling is very similar to that of the SSEs.

The cumulative aseismic slip in the region over the past twenty years can be estimated by adding together the slip produced by all SSEs and the cumulative slip under coupling regime. To estimate the slip deficit in the region, this total aseismic slip can then be compared with the average plate convergence of  $6.8 \pm 0.3$  cm/yr for the region (DeMets et al., 2010). Figure S7 shows the aseismic slip due to coupling and SSEs over 20 years separately. Subtracting the cumulative aseismic slip (i.e., the sum of both contributions) from the total distance of plate convergence (136 cm) for that period of time yields the slip deficit rate shown in Figure 8. This figure clearly shows a correlation between the maxima of the slip deficit rate and the rupture areas of large subduction thrust earthquakes. Since the coseismic signatures from the earthquakes have not been considered in this balance, the estimate is expressed as the slip deficit rate over the 20-year window. Biases in this calculation may arise from the overestimation of coupling-derived slip, as mentioned earlier, and from other possible factors discussed later.

### Figure 8

### 3. Discussion

#### 3.1. Mechanical transitions in the SSE habitat

As for the SSEs and coupling, the seismic radiation associated with slow slip (i.e. tremor, LFEs and repeaters) is also segmented in both states (see Figures 2, 3 and 4). In this instance, the segmentation primarily occurs along the plate interface dip, with radiation occurring at depths of less than 20 km, predominantly offshore, and at depths of more than 40 km, where long-term SSEs release less than ~40% of their seismic moment. This observation shows that regions where SSEs release the most elastic energy are seismically quiet (between 20 and 40 km), indicating that it is not possible to make inferences about the physics/intermittence of slip from seismic signals in these large regions. In addition, smaller, short-term SSEs have been observed in the seismically active regions, primarily in the down-dip area, where tremor and slow slip activity occur intermittently and in clusters over space and time (El Yousfi et al., 2023; Frank et al., 2018, 2016). The available evidence suggests that the regions where short-term SSEs and tremor coexist represent transition zones towards free slip. These regions are clearly located at the along-dip extremes where long-term SSEs vanish in both states (see Figures 3 and 4). In these zones, slow instabilities appear to transition from a state of significant size, quiescence, and continuity at depths ranging from 20 to 40 km, to a state of reduced size, intermittent occurrence, and tremor radiation above 20 km and below 40 km.

The observed behavioral differentiation within the SSEs' habitat appears to have a mechanical explanation in light of the results obtained. The dynamic condition  $(a - b)\sigma_{ss}$  at the interface indicates that, in accordance with theoretical rate and state friction models of SSEs in the region (Cruz-Atienza et al., 2021; Perez-Silva et al., 2021), the segment where long-term SSEs develop (between approximately 20 and 42 km) is characterized by velocity weakening friction (see Figures 3b, 4b, 5c). This means that the interface in this segment is inherently unstable, resulting in substantial, uninterrupted SSEs. At regions where short-term SSEs and tremor coexist, the interface transitions to a moderate velocity strengthening condition. This implies that slow instabilities in these regions are conditioned by externally-induced stress perturbations (see Figures 3b and 4b). In the case of Guerrero, the deep transition zone coincides with the so-called 'sweet spot' (Frank et al., 2013; A.L. Husker et al., 2012), where tremor emission is overwhelming and where overpressured fluids produce rapid tremor migration (Audet and Kim, 2016; Cruz-Atienza et al., 2018b; Frank et al., 2014; Manea and Manea, 2011). Therefore, it is a zone where the fault is weakest (i.e., where the effective pressure is lowest) and thus critically stressed by free slip at depth. Under these velocity-strengthening conditions, the normal stress is likely below the critical value at which the system transitions to unstable behavior giving rise to oscillatory instabilities and, consequently, intermittent slip and tremor (Scholz, 2018). A similar argument holds for the shallow VS transition zone, close to the oceanic trench, where lithostatic pressure is low and slow and repeating earthquakes are also observed.

#### 3.2. Stability in the Guerrero seismic gap

Of particular interest is the offshore zone along the Guerrero seismic gap, which experiences the highest values of  $(a - b)\sigma_{ss}$  in the entire region (see Figures 3b, 5c and S6). The plate interface in this segment between 10 and 20 km depth, is the most velocity strengthening and

thus intrinsically stable. This theoretical prediction suggests that large slip instabilities cannot initiate there. Note that this estimate is derived from the inversion of the regional coupling and the associated CFS (see Figure S5), which are particularly well resolved in the seismic gap (see Figures S3 and S4). However, they are not capable to resolve local heterogeneities. The recent discovery of slow instabilities in this offshore region (i.e., shallow SSEs), as revealed by seafloor geodetic observations (Cruz-Atienza et al., 2025b), demonstrates that such SSEs can indeed occur. One of these events initiated in close proximity to the oceanic trench and propagated down-dip for several months towards the hypocentral zone of the Mw7.0 Acapulco earthquake in September 2021, thereby triggering its rupture. Furthermore, recent studies using ocean bottom seismometer data have revealed tremor offshore (Chen et al., 2025; Plata-Martinez et al., 2021), which allowed the identification of a region devoid of seismic activity that was interpreted as a stable slip zone right in the middle of the velocity strengthening region (Plata-Martinez et al., 2021). The alignment of theoretical and observational results strongly suggests that the two main reasons for the absence of M7+ earthquakes in the seismic gap since 1911 (UNAM Seismology Group, 2015) are the occurrence of shallow SSEs (either short- or long-term) and the stable mechanical condition of most of the interface offshore. This condition may be associated with the presence of subducted bathymetry producing heterogeneities in the plate interface (Plata-Martinez et al., 2024; Wang and Bilek, 2011), as well as overpressured fluids at the plate contact due to the impermeable geology of the continental lower crust (Husker et al., 2018).

Available observational evidence from the Guerrero seismic gap indicates that major ruptures are unlikely to initiate there. However, theoretical predictions from realistic earthquake cycle models with enhanced weakening friction (i.e., with thermal pressurization of fault-zone fluids) indicate a different outcome based on much longer than observable periods (Lambert, 2024; Noda and Lapusta, 2013). These models demonstrate that regions where slip deficit is low (i.e., where several meters of slip can be accommodated aseismically) can indeed experience large dynamic ruptures with 5-10 meters of coseismic slip. In fact, these models suggest that SSEs occurrence in the seismic gap may indicate that the earthquake cycle is close to an end and that the plate interface is been loaded to quasi-static failure, which is a condition prone to failure in a future earthquake. The mechanical heterogeneity of the interface revealed by shallow SSEs in the gap, and the enhanced dynamic weakening of the interface driven by incoming large earthquakes, could imply the propagation of large ruptures across the seismic gap possibly with dynamic overshoots. This phenomenon was observed during the Tohoku-Oki megathrust earthquake in 2011 (Ide et al., 2011). To reach a conclusion regarding the feasibility of this scenario, an evaluation integrating all recent findings in this specific region is required.

### **3.3. Strain budget and large earthquakes**

Interplate coupling and SSEs represent the primary tectonic processes that shape continental plate deformation and, consequently, the occurrence of large earthquakes. There are three questions important to us: (1) to what extent are SSEs and coupling responsible for large ruptures? (2) how do these effects vary in space? and (3) what are the implications these effects have on the slip deficit? Figure 6 shows an estimate of the cumulative CFS over 20 years (i.e., between 2002 and 2022) due to both processes. Note that these are coarse approximations since the stress due to coupling (Figure 6a) was estimated based on the

assumption that this process operates continuously throughout the analysis period and thus is overestimated to some extent. Furthermore, to estimate the stress due to SSEs in Oaxaca (Figure 6b), it was assumed that events prior to 2017 (see Figure 1) were, on average, similar to the five SSEs inverted after that date (Cruz-Atienza et al., 2025a). The initial noteworthy outcome found in Figure 6 manifests at depths ranging from 30 to 40 km, where deformations resulting from coupling are largely balanced by recurrent SSEs throughout the region (Figure 7b). On the other hand, the coupling effect is a dominant factor in the seismic potential of the western and eastern regions (segments A and D). This can be better appreciated in Figure 7c, where it is also clear that the situation changes in segment C because both processes contribute similarly to that potential. In contrast, since downdip the Guerrero seismic gap (segment B) exhibits a high coupling coefficient (above 0.7) between 25 and 40 km depth (Figure 5b), the shallow CFS results in a pronounced stress shadow offshore (see Figure 6a). This effect is only partially compensated by the SSEs (see Figure 7c). In this instance, we note that the amplitude of the stress shadow may be overestimated, since the kinematic approach used to estimate the coupling pattern does not satisfy the elastostatic equations throughout the volume (Lindsey et al., 2021). However, based on our comprehensive analysis and on previous investigations (Cruz-Atienza et al., 2025b; Plata-Martinez et al., 2021; Radiguet et al., 2016; Rousset et al., 2016), we believe that a significant offshore region of the seismic gap acts predominantly as a stress-sinking area due to persistent, stable sliding, as argued previously.

As discussed by Cruz-Atienza et al. (2025a), the last six M7+ earthquakes around the states of Guerrero and Oaxaca were preceded and likely triggered by SSEs in most cases (see Figures 1 and 2 for earthquake location). This finding suggests that seismic hazard may rise during the occurrence of SSEs. However, a simple inspection of the Mexican historical record since the discovery in 1997 of the SSEs (Figure 1) reveals that the cluster of large earthquakes arises after a protracted 17-year quiescent period that began following the 1995 rupture of the Mw7.3 Copala earthquake (e.g., Courboux et al., 1997) (Figure 5a). This indicates that periodic SSEs in that quiet time frame did not trigger any major earthquake. Therefore, transient slow slip seems to be a necessary but insufficient process to initiate large ruptures. This particular pattern, in which earthquake clusters lasting approximately 15 years are preceded by a similar period of quiescence, has been observed in Mexico since 1800 (Singh et al., 1981) and suggests the existence of periodic regional loading and discharge of the subduction zone (Nocquet et al., 2016). During the active periods, the plate interface seismogenic segments appear to attain a state of critical stability in a synchronous manner, thereby rendering them susceptible to rupture triggered by perturbations from SSEs – as evidenced by observations spanning the period from 2012 to 2021 in Guerrero and Oaxaca.

### Table 1

The comprehensive SSE catalogue by Cruz-Atienza et al. (2025a) and the interplate coupling distribution we have developed made it possible to estimate the long-term slip deficit rate in the region (Figure 8). There are three clearly defined segments where long-term strain energy accumulates, and a fourth segment that appears to be non-seismogenic across the Guerrero seismic gap. The recent discovery of large (M7+) repeating earthquakes in south-central Mexico (Garza-Giron et al., 2025; Singh et al., 2024) allows an exercise to test our slip deficit model. The recurrence times of large subduction earthquakes in Mexico have been found to be inconsistent in specific segments (Singh et al., 1981). This indicates that three earthquakes

rupturing the same asperity can exhibit a variation in recurrence times of 10-18 years, as evidenced by the  $Mw7.4$  repeating sequence of 1928, 1965 and 2020 near Huatulco, eastern Oaxaca, and the  $Mw7.2$  sequence of 1928, 1968 and 2018 in Pinotepa Nacional, Oaxaca (Singh et al., 2024) (sequences b and d in Figure 8). If we assume the rupture area of these seismic events is given by  $A = 10^{M-3.99} \text{ km}^2$  (a robust estimate for subduction earthquakes in Mexico, Singh et al., 1980), then the average slip is given by  $\bar{d} = M_0 / [10^6 \cdot \mu \cdot A] \text{ m}$ , where  $\mu = 32^9 \text{ Pa}$  is the shear modulus,  $M$  the magnitude of the event and  $M_0$  its seismic moment in  $N \cdot \text{m}$ . Consequently, the average slip for the first and second sequences is  $\bar{d} = 1.93$  and  $1.53 \text{ m}$ , respectively. From Figure 8, the mean slip deficit rate in the rupture regions of these sequences is  $4.33$  and  $2.63 \text{ cm/yr}$  that, given the recurrence periods, yields predictions of  $1.99 \pm 0.55$  and  $1.14 \pm 0.18 \text{ m}$ , respectively, which are reasonably consistent with the  $\bar{d}$  estimates. The same exercise can be performed for the repeating earthquakes  $Mw7.6$  of 1928 and 1978 (sequence c), and for the succession of ruptures in the Papanao region  $Mw \sim 7.3$  of 1943, 1979 and 2014, west of the study region (sequence a). Table 1 provides a comparison of  $\bar{d}$  for each sequence with the predictions of the slip deficit model. Despite the model's tendency to underestimate predictions by an average of 14%, the observed consistency is noteworthy. This means that the slip deficit pattern found (Figure 8), which derives from the 20-year estimate of aseismic slip (Figure S7), is indeed reasonable for the region.

#### 4. Conclusions

Our findings indicate a strong agreement between the inter-SSE coupling pattern and multiple cycles of SSEs in both Guerrero and Oaxaca. As the SSEs, the coupling is also segmented along the plate interface strike with two maxima reaching values above 0.7 between 30 and 40 km depth (Figure 5b). In this depth range, the cumulative CFS over 20 years associated with coupling is overall balanced by the corresponding values of CFS due to SSEs (Figure 7b). At the borders of the study region (longitudes west of  $-101^\circ$  and east of  $-97.5^\circ$ ), where the effect of SSEs is negligible, coupling prevails in offshore areas (i.e. over 8-25 km depth), with values around 0.5, where large earthquakes have ruptured in the past (Figure 5a). The cumulative CFS in these segments is primarily due to coupling and fluctuates around 200 kPa over the last twenty years, with a more pronounced effect in Oaxaca, to the east (Figure 7c). Around the Guerrero-Oaxaca border, where significant seismic events have also been recorded (Figure 5a), the CFS seismogenic contributions from both coupling and SSEs are highly comparable, with cumulative values over the past two decades reaching approximately 100 kPa. In contrast, the Guerrero seismic gap has not shown any positive, seismogenic CFS over the same time period at interface depths between 8 and 25 km. All of these estimates disregard the coseismic effects of recent earthquakes, meaning they are only useful for distinguishing what controls the long-term stress accumulation.

Slow (i.e., tremor, LFEs and VLFs) and repeating earthquakes reported in the literature for Guerrero and Oaxaca feature a clear and consistent along-dip segmentation of seismic radiation associated with SSEs (see Figures 2, 3 and 4). These seismic sources concentrate above 20 km and below 40 km, where long-term SSEs fade out delivering only less than 40% of their seismic moment. This means that most regions where SSEs develop lack of seismic radiation, so nothing can be learned about the slow slip mechanics from seismic records. The dynamic condition  $(a - b)\sigma_{ss}$  of the plate interface reveals clear velocity weakening friction along these large SSE prone regions (with values below  $-0.2 \text{ MPa}$ ), which aligns with rate and



state friction SSE models for the region. As we approach the free-slip updip and downdip regions, friction becomes moderately velocity-strengthening (i.e. conditionally stable), where short-term SSEs, repeating and slow earthquakes concentrate (Figure 3 and 4), and overpressure fluids are present. The transition zones to free slip of the SSE habitat are thus characterized by weak normal stresses that, together with the free-slip shear loading, can potentially lead to system criticality producing oscillatory instabilities. These oscillations may help to explain the intermittent nature of slow slip as determined from seismic signals and the occurrence of short-term SSEs in these specific, bordering interface segments.

Offshore, the Guerrero seismic gap seems to be the most frictionally stable (i.e., velocity strengthening) segment in the whole region. However, slow slip instabilities (i.e., shallow and long-term SSEs) indeed happen in a large portion of the gap. This condition may indicate that the earthquake cycle is close to an end and that the plate interface is been loaded to quasi-static failure. The mechanical heterogeneity of the interface revealed by shallow SSEs, and the enhanced dynamic weakening of the interface driven by incoming large earthquakes, could allow the propagation of large ruptures across the seismic gap. In contrast, friction at both the western neighboring segment (where multiple earthquakes have occurred, Figure 5a) and the easternmost segment of the study region (i.e. longitudes east from -97.5°), where a ~M8.6 occurred in 1787 (Suárez and Albin, 2009), are intrinsically unstable (i.e. velocity weakening). In these two regions, both the cumulative CFS over the last two decades (Figure 7c) and the slip deficit rate (Figure 8) are the largest, suggesting that significant ruptures are likely to occur in the future. Consistent with large (M7+) repeating earthquake in the region (Singh et al., 2024), the interplate slip deficit delineates three distinct segments at seismogenic depths where strain energy accumulates over time. These are the two above mentioned extremes of the studied domain, and a third around the Guerrero-Oaxaca state boundary (Figure 8).

The Mexican seismic record since 1800 demonstrates that large seismic events tend to occur in clusters approximately every 15 years (Singh et al., 1981). Since 2012, when the current cluster began after 17 years of quiescence (Figure 1), SSEs have likely triggered five of the six M7+ earthquakes recorded in Guerrero and Oaxaca. As discussed by Cruz-Atienza et al. (2025a), this suggests that SSEs become large-earthquake triggers periodically, every time the subduction zone reaches a critically stressed condition in a synchronous manner.

#### **Declaration of competing interest**

The authors declare no conflicts of interest relevant to this study.

#### **Acknowledgments**

This research was possible thanks to UNAM PAPIIT grants IN111524, IA105725, IA104525 and IN107524. This work was supported by JST SATREPS Japan Grant Number JPMJSA2310.

#### **References**

Aguilar-Velázquez, M.J., Miranda-García, P., Cruz-Atienza, V.M., Solano-Rojas, D., Tago, J., Domínguez, L.A., Villafuerte, C., Espíndola, V.H., Bello-Segura, D., Quintanar-Robles, L., Pertou, M., 2025. Interplay of slow-slip faults beneath Mexico City induces intense



564 seismicity over months. *Tectonophysics* 902, 230659.  
<https://doi.org/10.1016/J.TECTO.2025.230659>

566 Audet, P., Kim, Y.H., 2016. Teleseismic constraints on the geological environment of deep  
 episodic slow earthquakes in subduction zone forearcs: a review. *Tectonophysics* 670, 1–  
 568 15. <https://doi.org/10.1016/j.tecto.2016.01.005>

Brudzinski, M., Cabral-Cano, E., Correa-Mora, F., Demets, C., Márquez-Azúa, B., 2007. Slow  
 570 slip transients along the Oaxaca subduction segment from 1993 to 2007. *Geophys. J. Int.*  
 171, 523–538. <https://doi.org/10.1111/j.1365-246x.2007.03542.x>

572 Brudzinski, M.R., Hinojosa-Prieto, H.R., Schlanser, K.M., Cabral-Cano, E., Arciniega-Ceballos,  
 A., Diaz-Molina, O., DeMets, C., 2010. Nonvolcanic tremor along the Oaxaca segment of  
 574 the Middle America subduction zone. *J Geophys Res Solid Earth* 115.  
<https://doi.org/10.1029/2008JB006061>

576 Cabral-Cano, E., Pérez-Campos, X., Márquez-Azúa, B., Sergeeva, M.A., Salazar-Tlaczani, L.,  
 DeMets, C., Adams, D., Galetzka, J., Hodgkinson, K., Feaux, K., Serra, Y.L., Mattioli, G.S.,  
 578 Miller, M., 2018. TLALOCNet: a continuous GPS-Met Backbone in Mexico for  
 seismotectonic and atmospheric research. *Seismol. Res. Lett.* 89, 373–381.  
 580 <https://doi.org/10.1785/0220170190>

Cavalié, O., Pathier, E., Radiguet, M., Vergnolle, M., Cotte, N., Walpersdorf, A., Kostoglodov,  
 582 V., Cotton, F., 2013. Slow slip event in the Mexican subduction zone: Evidence of  
 shallower slip in the Guerrero seismic gap for the 2006 event revealed by the joint  
 584 inversion of InSAR and GPS data. *Earth Planet Sci Lett* 367, 52–60.  
<https://doi.org/10.1016/J.EPSL.2013.02.020>

586 Chen, Y., Ito, Y., Plata-Martinez, R., Dominguez, L.A., Ohyanagi, S., Garcia, E.S., Flores, K., Cruz-  
 Atienza, V.M., Shinohara, M., Yamashita, Y., 2025. New insight into slow earthquake  
 588 activities from continuous ocean bottom seismometers at the Guerrero seismic gap,  
 Mexico. *Geophys J Int* 241, 511–525. <https://doi.org/10.1093/GJI/GGAF057>

590 Chlieh, M., Perfettini, H., Tavera, H., Avouac, J.P., Remy, D., Nocquet, J.M., Rolandone, F.,  
 Bondoux, F., Gabalda, G., Bonvalot, S., 2011. Interseismic coupling and seismic potential  
 592 along the Central Andes subduction zone. *J Geophys Res Solid Earth* 116.  
<https://doi.org/10.1029/2010JB008166>

594 Correa-Mora, F., DeMets, C., Cabral-Cano, E., Diaz-Molina, O., Marquez-Azua, B., 2009.  
 Transient deformation in southern Mexico in 2006 and 2007: Evidence for distinct deep-  
 596 slip patches beneath Guerrero and Oaxaca. *Geochemistry, Geophysics, Geosystems* 10.  
<https://doi.org/10.1029/2008GC002211>

598 Correa-Mora, F., Demets, C., Cabral-Cano, E., Marquez-Azua, B., Diaz-Molina, O., 2008.  
 Interplate coupling and transient slip along the subduction interface beneath Oaxaca,  
 600 Mexico. *Geophys J Int* 175, 269–290. <https://doi.org/10.1111/J.1365-246X.2008.03910.X/3/175-1-269-FIG017.JPEG>

602 Courboux, F., Santoyo, M.A., Pacheco, J.F., Singh, S.K., 1997. The 14 September 1995 (M =  
 7.3) Copala, Mexico, earthquake: A source study using teleseismic, regional, and local  
 604 data. *Bulletin of the Seismological Society of America* 87, 999–1010.  
<https://doi.org/10.1785/BSSA0870040999>

606 Cruz-Atienza, V.M., Frano, S., Kostoglodov, V., Tago, J., Kazachkina, E., Real, J., Villafuerte, C.,  
 Plata-Martínez, R., 2025a. Slow Slip Events in Mexico: A Historical Perspective.  
 608 *EarthArXiv*. <https://doi.org/10.31223/X5H740>.

Cruz-Atienza, V.M., Husker, A., Legrand, D., Caballero, E., Kostoglodov, V., 2015. Nonvolcanic  
 610 tremor locations and mechanisms in Guerrero, Mexico, from energy-based and particle

motion polarization analysis. *J Geophys Res Solid Earth* 120.

<https://doi.org/10.1002/2014JB011389>

Cruz-Atienza, V.M., Ito, Y., Kostoglodov, V., Hjörleifsdóttir, V., Iglesias, A., Tago, J., Calò, M.,  
Real, J., Husker, A., Ide, S., Nishimura, T., Shinohara, M., Mortera-Gutierrez, C., García, S.,  
Kido, M., 2018a. A seismogeodetic amphibious network in the Guerrero Seismic Gap,  
Mexico. *Seismological Research Letters* 89. <https://doi.org/10.1785/0220170173>

Cruz-Atienza, V.M., Tago, J., Domínguez, L.A., Kostoglodov, V., Ito, Y., Ovando-Shelley, E., et al.,  
2025b. Seafloor Geodesy Unveils Seismogenesis of Large Subduction Earthquakes in  
México. Under review in *Science Advances* 1–39.

Cruz-Atienza, V.M., Tago, J., Villafuerte, C., Wei, M., Garza-Girón, R., Dominguez, L.A.,  
Kostoglodov, V., Nishimura, T., Franco, S.I., Real, J., Santoyo, M.A., Ito, Y., Kazachkina, E.,  
2021. Short-term interaction between silent and devastating earthquakes in Mexico. *Nat*  
*Commun* 12. <https://doi.org/10.1038/s41467-021-22326-6>

Cruz-Atienza, V.M., Villafuerte, C., Bhat, H.S., 2018b. Rapid tremor migration and pore-  
pressure waves in subduction zones. *Nat Commun* 9. <https://doi.org/10.1038/s41467-018-05150-3>

DeMets, C., Gordon, R.G., Argus, D.F., 2010. Geologically current plate motions. *Geophys J.*  
*Int* 181, 1–80. <https://doi.org/10.1111/j.1365-246x.2009.04491.x>

Dieterich, J.H., 1979. Modeling of rock friction: 1. Experimental results and constitutive  
equations. *J Geophys Res Solid Earth* 84, 2161–2168.  
<https://doi.org/10.1029/JB084IB05P02161>

Dominguez, L.A., Taira, T., Cruz-Atienza, V.M., Iglesias, A., Villafuerte, C., Legrand, D., Pérez-  
Campos, X., Raggi, M., 2022. Interplate Slip Rate Variation Between Closely Spaced  
Earthquakes in Southern Mexico: The 2012 Ometepc and 2018 Pinotepa Nacional  
Thrust Events. *J Geophys Res Solid Earth* 127, e2022JB024292.  
<https://doi.org/10.1029/2022JB024292>

Dominguez, L.A., Taira, T., Santoyo, M.A., 2016. Spatiotemporal variations of characteristic  
repeating earthquake sequences along the Middle America Trench in Mexico. *J Geophys*  
*Res Solid Earth* 121, 8855–8870. <https://doi.org/10.1002/2016JB013242>

El Yousfi, Z., Radiguet, M., Rousset, B., Husker, A., Kazachkina, E., Kostoglodov, V., 2023.  
Intermittence of transient slow slip in the Mexican subduction zone. *Earth Planet Sci*  
*Lett* 620, 118340. <https://doi.org/10.1016/J.EPSL.2023.118340>

Franco, S.I., Kostoglodov, V., Larson, K.M., Manea, V.C., Manea, M., Santiago, J.A., 2005.  
Propagation of the 2001-2002 silent earthquake and interplate coupling in the Oaxaca  
subduction zone, Mexico. *Earth, Planets and Space* 57, 973–985.  
<https://doi.org/10.1186/BF03351876/METRICS>

Frank, W.B., Radiguet, M., Rousset, B., Shapiro, N.M., Husker, A.L., Kostoglodov, V., Cotte, N.,  
Campillo, M., 2015. Uncovering the geodetic signature of silent slip through repeating  
earthquakes. *Geophys Res Lett* 42, 2774–2779. <https://doi.org/10.1002/2015GL063685>

Frank, W.B., Rousset, B., Lasserre, C., Campillo, M., 2018. Revealing the cluster of slow  
transients behind a large slow slip event. *Sci Adv* 4.  
<https://doi.org/10.1126/SCIADV.AAT0661>

Frank, W.B., Shapiro, N.M., Husker, A.L., Kostoglodov, V., Gusev, A.A., Campillo, M., 2016. The  
evolving interaction of low-frequency earthquakes during transient slip. *Sci Adv* 2.  
[https://doi.org/10.1126/SCIADV.1501616/SUPPL\\_FILE/1501616\\_SM.PDF](https://doi.org/10.1126/SCIADV.1501616/SUPPL_FILE/1501616_SM.PDF)

Frank, W.B., Shapiro, N.M., Husker, A.L., Kostoglodov, V., Romanenko, A., Campillo, M., 2014.  
Using systematically characterized low-frequency earthquakes as a fault probe in

Guerrero, Mexico. *J Geophys Res Solid Earth* 119, 7686–7700.  
<https://doi.org/10.1002/2014JB011457>

Frank, W.B., Shapiro, N.M., Kostoglodov, V., Husker, A.L., Campillo, M., Payero, J.S., Prieto, G.A., 2013. Low-frequency earthquakes in the Mexican sweet spot. *Geophys Res Lett* 40, 2661–2666. <https://doi.org/10.1002/GRL.50561>

Garza-Giron, R., Lay, T., Ye, L., 2025. The Repeating Major Earthquakes in the Mexican Subduction Zone Along Oaxaca: Implications for Future Events. *Seismological Research Letters* 96, 1548–1560. <https://doi.org/10.1785/0220240267>

Graham, S., DeMets, C., Cabral-Cano, E., Kostoglodov, V., Rousset, B., Walpersdorf, A., Cotte, N., Lasserre, C., McCaffrey, R., Salazar-Tlaczani, L., 2016. Slow Slip History for the MEXICO Subduction Zone: 2005 Through 2011. *Pure Appl. Geophys.* 173, 3445–3465. <https://doi.org/10.1007/s00024-015-1211-x>

Graham, S.E., DeMets, C., Cabral-Cano, E., Kostoglodov, V., Walpersdorf, A., Cotte, N., Brudzinski, M., McCaffrey, R., Salazar-Tlaczani, L., 2014. GPS constraints on the 2011–2012 Oaxaca slow slip event that preceded the 2012 March 20 Ometepepec earthquake, southern Mexico. *Geophys J Int* 197, 1593–1607. <https://doi.org/10.1093/GJI/GGU019>

Hsu, Y.J., Simons, M., Avouac, J.P., Galetka, J., Sieh, K., Chlieh, M., Natawidjaja, D., Prawirodirdjo, L., Bock, Y., 2006. Frictional afterslip following the 2005 Nias-Simeulue earthquake, Sumatra. *Science* (1979) 312, 1921–1926. [https://doi.org/10.1126/SCIENCE.1126960/SUPPL\\_FILE/HSU.SOM.PDF](https://doi.org/10.1126/SCIENCE.1126960/SUPPL_FILE/HSU.SOM.PDF)

Husker, A., Ferrari, L., Arango-Galván, C., Corbo-Camargo, F., Arzate-Flores, J.A., 2018. A geologic recipe for transient slip within the seismogenic zone: Insight from the Guerrero seismic gap, Mexico. *Geology* 46, 35–38. <https://doi.org/10.1130/G39202.1>

Husker, A.L., Kostoglodov, V., Cruz-Atienza, V.M., Legrand, D., Shapiro, N.M., Payero, J.S., Campillo, M., Huesca-Pérez, E., 2012. Temporal variations of non-volcanic tremor (NVT) locations in the Mexican subduction zone: Finding the NVT sweet spot. *Geochemistry, Geophysics, Geosystems* 13. <https://doi.org/10.1029/2011GC003916>

Ide, S., Baltay, A., Beroza, G.C., 2011. Shallow dynamic overshoot and energetic deep rupture in the 2011 M w 9.0 Tohoku-Oki earthquake. *Science* (1979) 332, 1426–1429. [https://doi.org/10.1126/SCIENCE.1207020/SUPPL\\_FILE/1207020-IDE-SOM.PDF](https://doi.org/10.1126/SCIENCE.1207020/SUPPL_FILE/1207020-IDE-SOM.PDF)

Iglesias, A., Singh, S.K., Lowry, A.R., Santoyo, M., Kostoglodov, V., Larson, K.M., Franco-Sánchez, S.I., 2004. The silent earthquake of 2002 in the Guerrero seismic gap, Mexico (Mw=7.6): Inversion of slip on the plate interface and some implications. *Geofísica Internacional* 43, 309–317. <https://doi.org/10.22201/IGEOF.00167169P.2004.43.3.953>

Jolivet, R., Frank, W.B., 2020. The Transient and Intermittent Nature of Slow Slip. *AGU Advances* 1, e2019AV000126. <https://doi.org/10.1029/2019AV000126>

Kostoglodov, V., Husker, A., Shapiro, N.M., Payero, J.S., Campillo, M., Cotte, N., Clayton, R., 2010. The 2006 slow slip event and nonvolcanic tremor in the Mexican subduction zone. *Geophys Res Lett* 37. <https://doi.org/10.1029/2010GL045424>

Kostoglodov, V., Singh, S.K., Santiago, J.A., Franco, S.I., Larson, K.M., Lowry, A.R., Bilham, R., 2003. A large silent earthquake in the Guerrero seismic gap, Mexico. *Geophys Res Lett* 30. <https://doi.org/10.1029/2003GL017219>

Lambert, V., 2024. Slow Slip as an Indicator of Fault Stress Criticality. *Geophys Res Lett* 51, e2023GL107356. <https://doi.org/10.1029/2023GL107356>

Lindsey, E.O., Mallick, R., Hubbard, J.A., Bradley, K.E., Almeida, R. V., Moore, J.D.P., Bürgmann, R., Hill, E.M., 2021. Slip rate deficit and earthquake potential on shallow megathrusts.

704 Nature Geoscience 2021 14:5 14, 321–326. [https://doi.org/10.1038/s41561-021-00736-](https://doi.org/10.1038/s41561-021-00736-x)  
 x  
 706 Liu, Y., Rice, J.R., 2005. Aseismic slip transients emerge spontaneously in three-dimensional  
 rate and state modeling of subduction earthquake sequences. *J Geophys Res Solid Earth*  
 708 110, 1–14. <https://doi.org/10.1029/2004JB003424>  
 Lowry, A.R., Larson, K.M., Kostoglodov, V., Bilham, R., 2001. Transient fault slip in Guerrero,  
 710 southern Mexico. *Geophys Res Lett* 28, 3753–3756.  
<https://doi.org/10.1029/2001GL013238>  
 712 Manea, V.C., Manea, M., 2011. Flat-slab thermal structure and evolution beneath central  
 Mexico. *Pure Appl Geophys* 168, 1475–1487. [https://doi.org/10.1007/S00024-010-](https://doi.org/10.1007/S00024-010-0207-9/FIGURES/6)  
 714 0207-9/FIGURES/6  
 Martínez-López, M.R., Suárez, G., Mendoza, C., 2025. Rupture zones of the 1978 (Mw 7.6)  
 716 and 2020 (Mw 7.4) earthquakes in the Oaxaca subduction zone: Implications for seismic  
 slip and seismic hazard. *J Seismol* 29, 317–336. [https://doi.org/10.1007/S10950-024-](https://doi.org/10.1007/S10950-024-10275-8/TABLES/5)  
 718 10275-8/TABLES/5  
 Maury, J., Ide, S., Cruz-Atienza, V.M., Kostoglodov, V., 2018. Spatiotemporal Variations in Slow  
 720 Earthquakes Along the Mexican Subduction Zone. *J Geophys Res Solid Earth* 123.  
<https://doi.org/10.1002/2017JB014690>  
 722 Maury, J., Ide, S., Cruz-Atienza, V.M., Kostoglodov, V., González-Molina, G., Pérez-Campos, X.,  
 2016. Comparative study of tectonic tremor locations: Characterization of slow  
 724 earthquakes in Guerrero, Mexico. *J Geophys Res Solid Earth* 121, 5136–5151.  
 Nikkhoo, M., Walter, T.R., 2015. Triangular dislocation: an analytical, artefact-free solution.  
 726 *Geophys J Int* 201, 1119–1141. <https://doi.org/10.1093/GJI/GGV035>  
 Nishikawa, T., Ide, S., Nishimura, T., 2023. A review on slow earthquakes in the Japan Trench.  
 728 *Progress in Earth and Planetary Science* 2022 10:1 10, 1–51.  
<https://doi.org/10.1186/S40645-022-00528-W>  
 730 Nocquet, J.M., Jarrin, P., Vallée, M., Mothes, P.A., Grandin, R., Rolandone, F., Delouis, B.,  
 Yepes, H., Font, Y., Fuentes, D., Régnier, M., Laurendeau, A., Cisneros, D., Hernandez, S.,  
 732 Sladen, A., Singaicho, J.C., Mora, H., Gomez, J., Montes, L., Charvis, P., 2016. Supercycle  
 at the Ecuadorian subduction zone revealed after the 2016 Pedernales earthquake.  
 734 *Nature Geoscience* 2017 10:2 10, 145–149. <https://doi.org/10.1038/ngeo2864>  
 Noda, H., Lapusta, N., 2013. Stable creeping fault segments can become destructive as a  
 736 result of dynamic weakening. *Nature* 2013 493:7433 493, 518–521.  
<https://doi.org/10.1038/nature11703>  
 738 Obara, K., Hirose, H., Yamamizu, F., Kasahara, K., 2004. Episodic slow slip events accompanied  
 by non-volcanic tremors in southwest Japan subduction zone. *Geophys Res Lett* 31, 1–4.  
 740 <https://doi.org/10.1029/2004GL020848>  
 Obara, K., Kato, A., 2016. Connecting slow earthquakes to huge earthquakes. *Science* (1979)  
 742 353, 253–257. <https://doi.org/10.1126/science.aaf1512>  
 Payero, J.S., Kostoglodov, V., Shapiro, N., Mikumo, T., Iglesias, A., Pérez-Campos, X., Clayton,  
 744 R.W., 2008. Nonvolcanic tremor observed in the Mexican subduction zone. *Geophys Res*  
*Lett* 35. <https://doi.org/10.1029/2007GL032877>  
 746 Perez-Silva, A., Li, D., Gabriel, A.A., Kaneko, Y., 2021. 3D Modeling of Long-Term Slow Slip  
 Events Along the Flat-Slab Segment in the Guerrero Seismic Gap, Mexico. *Geophys Res*  
 748 *Lett* 48, e2021GL092968. <https://doi.org/10.1029/2021GL092968>  
 Plata-Martinez, R., Ide, S., Shinohara, M., Garcia, E.S., Mizuno, N., Dominguez, L.A., Taira, T.,  
 750 Yamashita, Y., Toh, A., Yamada, T., Real, J., Husker, A., Cruz-Atienza, V.M., Ito, Y., 2021.

Shallow slow earthquakes to decipher future catastrophic earthquakes in the Guerrero seismic gap. *Nat Commun* 12. <https://doi.org/10.1038/S41467-021-24210-9>

Plata-Martinez, R., Iinuma, T., Tomita, F., Nakamura, Y., Nishimura, T., Hori, T., 2024. Revisiting Slip Deficit Rates and Its Insights Into Large and Slow Earthquakes at the Nankai Subduction Zone. *J Geophys Res Solid Earth* 129, e2023JB027942. <https://doi.org/10.1029/2023JB027942>

Radiguet, M., Cotton, F., Vergnolle, M., Campillo, M., Valette, B., Kostoglodov, V., Cotte, N., 2011. Spatial and temporal evolution of a long term slow slip event: The 2006 Guerrero Slow Slip Event. *Geophys J Int* 184, 816–828. <https://doi.org/10.1111/J.1365-246X.2010.04866.X>

Radiguet, M., Cotton, F., Vergnolle, M., Campillo, M., Walpersdorf, A., Cotte, N., Kostoglodov, V., 2012. Slow slip events and strain accumulation in the Guerrero gap, Mexico. *J Geophys Res Solid Earth* 117. <https://doi.org/10.1029/2011JB008801>

Radiguet, M., Perfettini, H., Cotte, N., Gualandi, A., Valette, B., Kostoglodov, V., Lhomme, T., Walpersdorf, A., Cabral Cano, E., Campillo, M., 2016. Triggering of the 2014 Mw7.3 Papanao earthquake by a slow slip event in Guerrero, Mexico. *Nat. Geosci.* 9, 829–833. <https://doi.org/10.1038/ngeo2817>

Rogers, G., Dragert, H., 2003. Episodic tremor and slip on the Cascadia subduction zone: The chatter of silent slip. *Science* (1979) 300, 1942–1943. <https://doi.org/10.1126/SCIENCE.1084783>

Rousset, B., Campillo, M., Lasserre, C., Frank, W.B., Cotte, N., Walpersdorf, A., Socquet, A., Kostoglodov, V., 2017. A geodetic matched filter search for slow slip with application to the Mexico subduction zone. *J Geophys Res Solid Earth* 122, 10,498–10,514. <https://doi.org/10.1002/2017JB014448>

Rousset, B., Lasserre, C., Cubas, N., Graham, S., Radiguet, M., DeMets, C., Socquet, A., Campillo, M., Kostoglodov, V., Cabral-Cano, E., Cotte, N., Walpersdorf, A., 2016. Lateral Variations of Interplate Coupling along the Mexican Subduction Interface: Relationships with Long-Term Morphology and Fault Zone Mechanical Properties. *Pure Appl Geophys* 173, 3467–3486. <https://doi.org/10.1007/S00024-015-1215-6/FIGURES/10>

Ruina, A., 1983. Slip instability and state variable friction laws. *J Geophys Res Solid Earth* 88, 10359–10370. <https://doi.org/10.1029/JB088IB12P10359>

Scholz, C.H., 2018. *The Mechanics of Earthquakes and Faulting*, The Mechanics of Earthquakes and Faulting, 3rd Edition. Cambridge University Press. <https://doi.org/10.1017/9781316681473>

Singh, S.K., Astiz, L., Havskov, J., 1981. Seismic gaps and recurrence periods of large earthquakes along the Mexican subduction zone: A reexamination. *Bulletin of the Seismological Society of America* 71, 827–843. <https://doi.org/10.1785/BSSA0710030827>

Singh, S.K., Bazan, E., Esteva, L., 1980. Expected earthquake magnitude from a fault. *Bulletin of the Seismological Society of America* 70, 903–914. <https://doi.org/10.1785/BSSA0700030903>

Singh, S.K., Corona-Fernandez, R.D., Santoyo, M.Á., Iglesias, A., 2024. Repeating Large Earthquakes along the Mexican Subduction Zone. *Seismological Research Letters* 95, 458–478. <https://doi.org/10.1785/0220230243>

Tago, J., Cruz-Atienza, V.M., Villafuerte, C., Nishimura, T., Kostoglodov, V., Real, J., Ito, Y., 2021. Adjoint slip inversion under a constrained optimization framework: Revisiting the 2006 Guerrero slow slip event. *Geophys J Int* 226. <https://doi.org/10.1093/gji/ggab165>

798 UNAM Seismology Group, 2015. Papanao, Mexico earthquake of 18 April 2014 (Mw7.3).  
 Geofisica Internacional 54, 363–386.

800 Vergnolle, M., Walpersdorf, A., Kostoglodov, V., Tregoning, P., Santiago, J.A., Cotte, N., Franco,  
 S.I., 2010. Slow slip events in Mexico revised from the processing of 11 year GPS  
 802 observations. *J Geophys Res Solid Earth* 115, 8403.  
<https://doi.org/10.1029/2009JB006852>

804 Villafuerte, C., Cruz-Atienza, V.M., 2017. Insights into the causal relationship between slow  
 slip and tectonic tremor in Guerrero, Mexico. *J Geophys Res Solid Earth* 122, 6642–  
 806 6656.

Villafuerte, C., Cruz-Atienza, V.M., Tago, J., Solano-Rojas, D., Garza-Girón, R., Girón, G.,  
 808 Franco, S.I., Dominguez, L.A., Kostoglodov, V., 2025. Slow slip events and megathrust  
 coupling changes contribute to the earthquake potential in Oaxaca, Mexico. *Geophys J*  
 810 *Int* 241, 17–34. <https://doi.org/10.1093/GJI/GGAF022>

Walpersdorf, A., Cotte, N., Kostoglodov, V., Vergnolle, M., Radiguet, M., Santiago, J.A.,  
 812 Campillo, M., 2011. Two successive slow slip events evidenced in 2009–2010 by a dense  
 GPS network in Guerrero, Mexico. *Geophys Res Lett* 38.  
 814 <https://doi.org/10.1029/2011GL048124>

Wang, K., Bilek, S.L., 2011. Do subducting seamounts generate or stop large earthquakes?  
 816 *Geology* 39, 819–822. <https://doi.org/10.1130/G31856.1>

Weiss, J.R., Qiu, Q., Barbot, S., Wright, T.J., Foster, J.H., Saunders, A., Brooks, B.A., Bevis, M.,  
 818 Kendrick, E., Ericksen, T.L., Avery, J., Smalley, R.S., Cimbaro, S.R., Lenzano, L.E., Barón, J.,  
 Báez, J.C., Echalar, A., 2019. Illuminating subduction zone rheological properties in the  
 820 wake of a giant earthquake. *Sci Adv* 5, 6720–6738.  
[https://doi.org/10.1126/SCIADV.AAX6720/SUPPL\\_FILE/AAX6720\\_SM.PDF](https://doi.org/10.1126/SCIADV.AAX6720/SUPPL_FILE/AAX6720_SM.PDF)

822

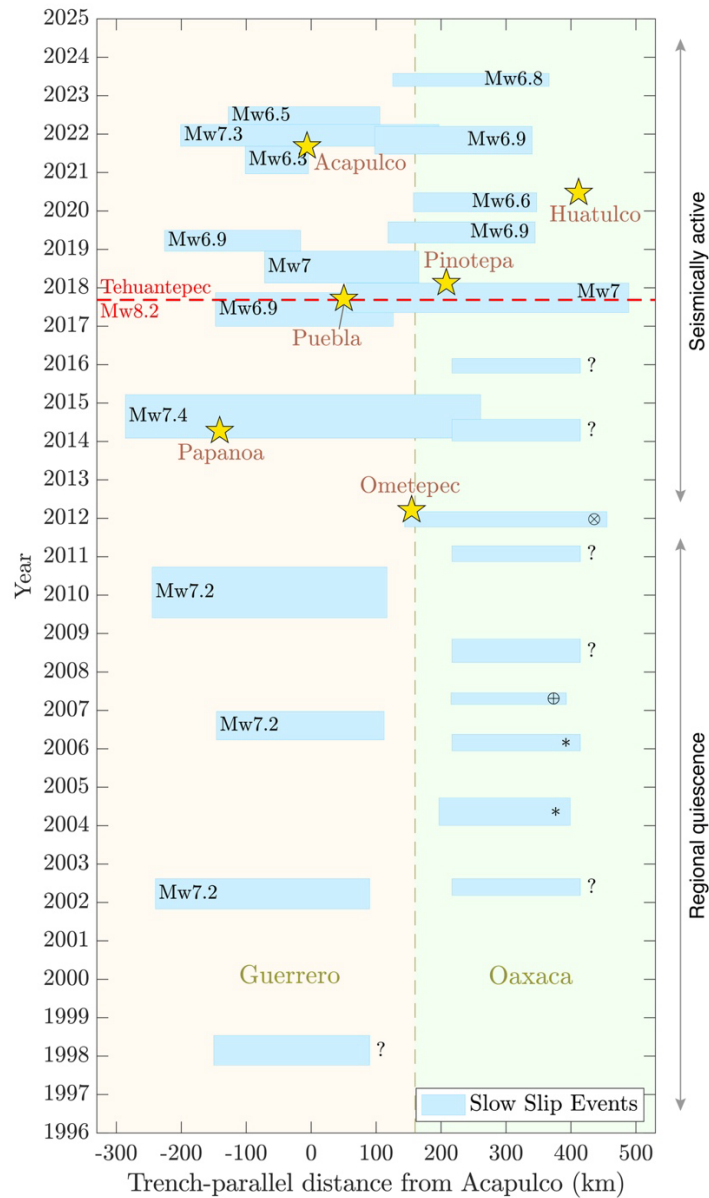


**Figure 1** Temporal distribution in the trench-parallel direction from Acapulco of all known SSEs and M7+ earthquakes in Guerrero and Oaxaca. Events with indicated magnitudes were inverted for the slip distribution. The duration of SSEs with a question mark was determined from GPS records in Oaxaca, while their extent is only indicative. SSEs indicated with an asterisk (\*) are from Correa-Mora et al. (2008), those annotated with the symbol ⊗ are from Correa-Mora et al. (2009), and those with the symbol ⊕ are from Graham et al. (2014). The figure is modified from Cruz-Atienza et al. (2025a).

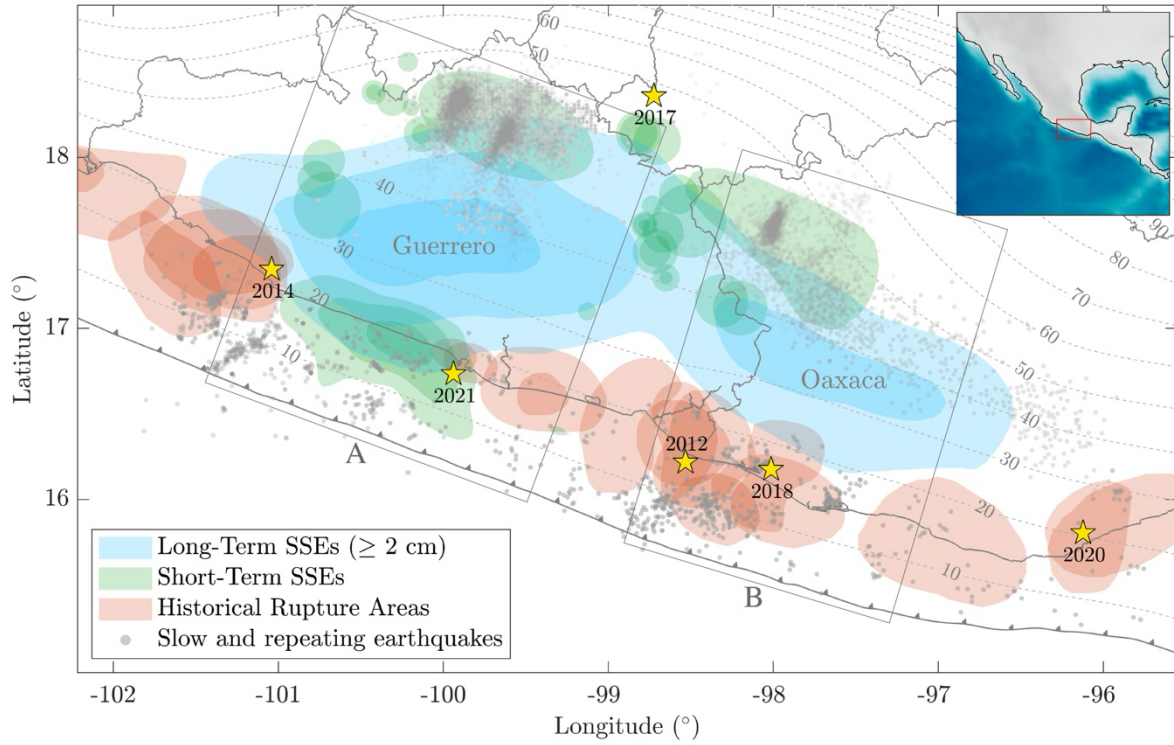


**Figure 2** Distribution of short-term SSEs (Cruz-Atienza et al., 2025b; El Yousfi et al., 2023; Frank et al., 2015; Rousset et al., 2017; Villafuerte and Cruz-Atienza, 2017), slow (i.e. tremor and LFEs) and repeating earthquakes (Brudzinski et al., 2010; Chen et al., 2025; Dominguez et al., 2022; Frank et al., 2014; Maury et al., 2018; Plata-Martinez et al., 2021; Villafuerte and Cruz-Atienza, 2017) available in the literature. The long-term SSE average slip determined by Cruz-Atienza et al. (2025a) is shown as blue shades. Trench-parallel average profiles along the A and B rectangles are shown in Figures 3 and 4, respectively.



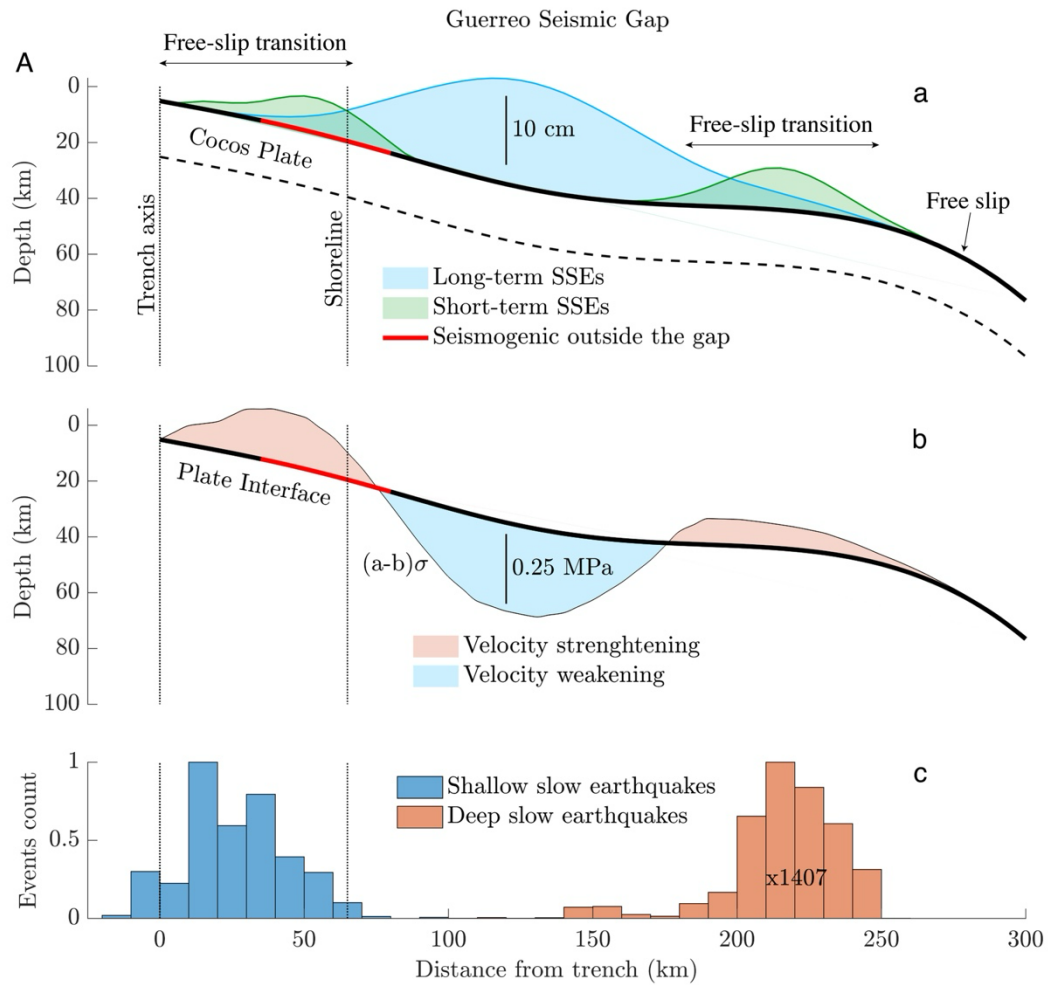


**Figure 3** Average cross-section over region A (Figure 2) of different SSE-related matters. (a) average slow slip distribution for long- and short-term SSEs along the plate interface (black curve). Amplitude of the short-term SSEs is arbitrarily scaled to better appreciate their locations. (b) Distribution along the plate interface of the dynamic condition  $(a - b)\sigma_{ss}$  (see Figure 6c). (c) Normalized histograms of tremor, LFEs and repeating earthquakes reported in the literature.

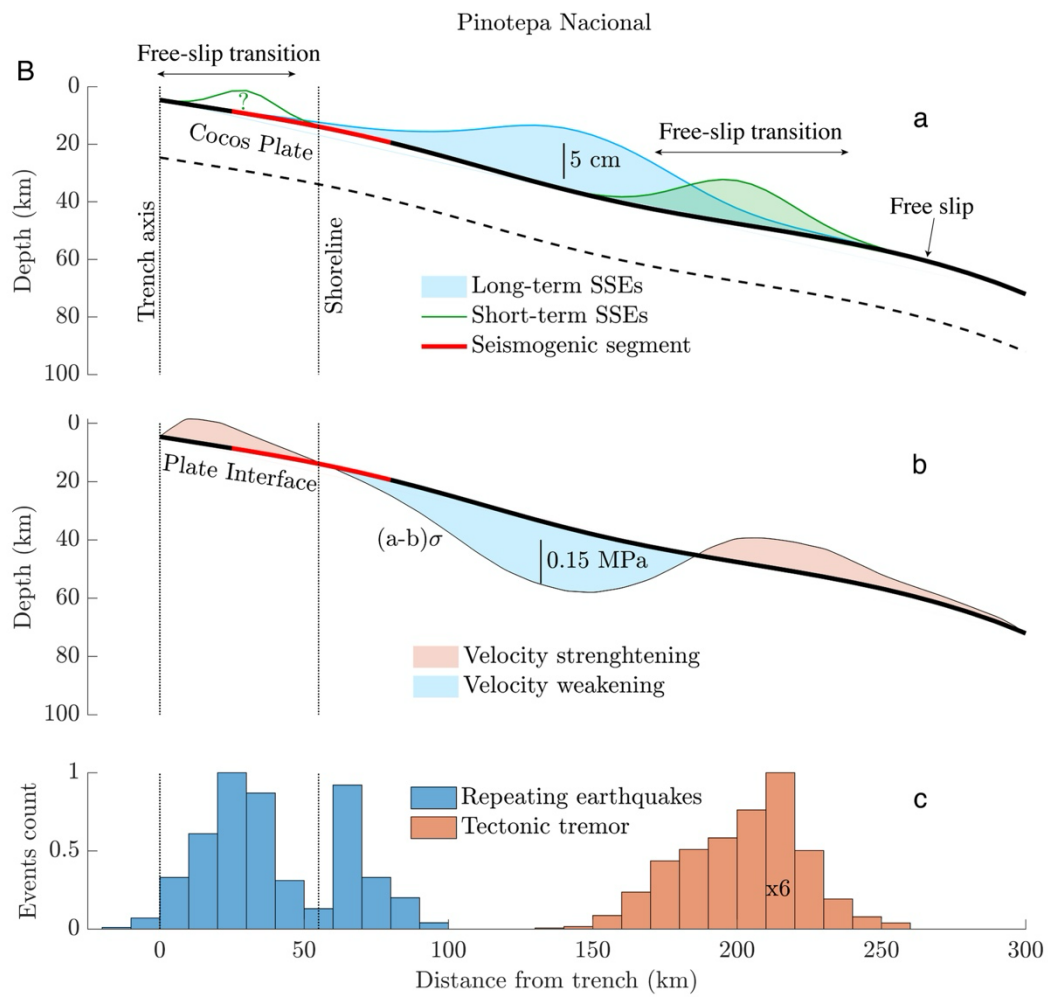


**Figure 4** Same as Figure 3 but over region B indicated in Figure 2.

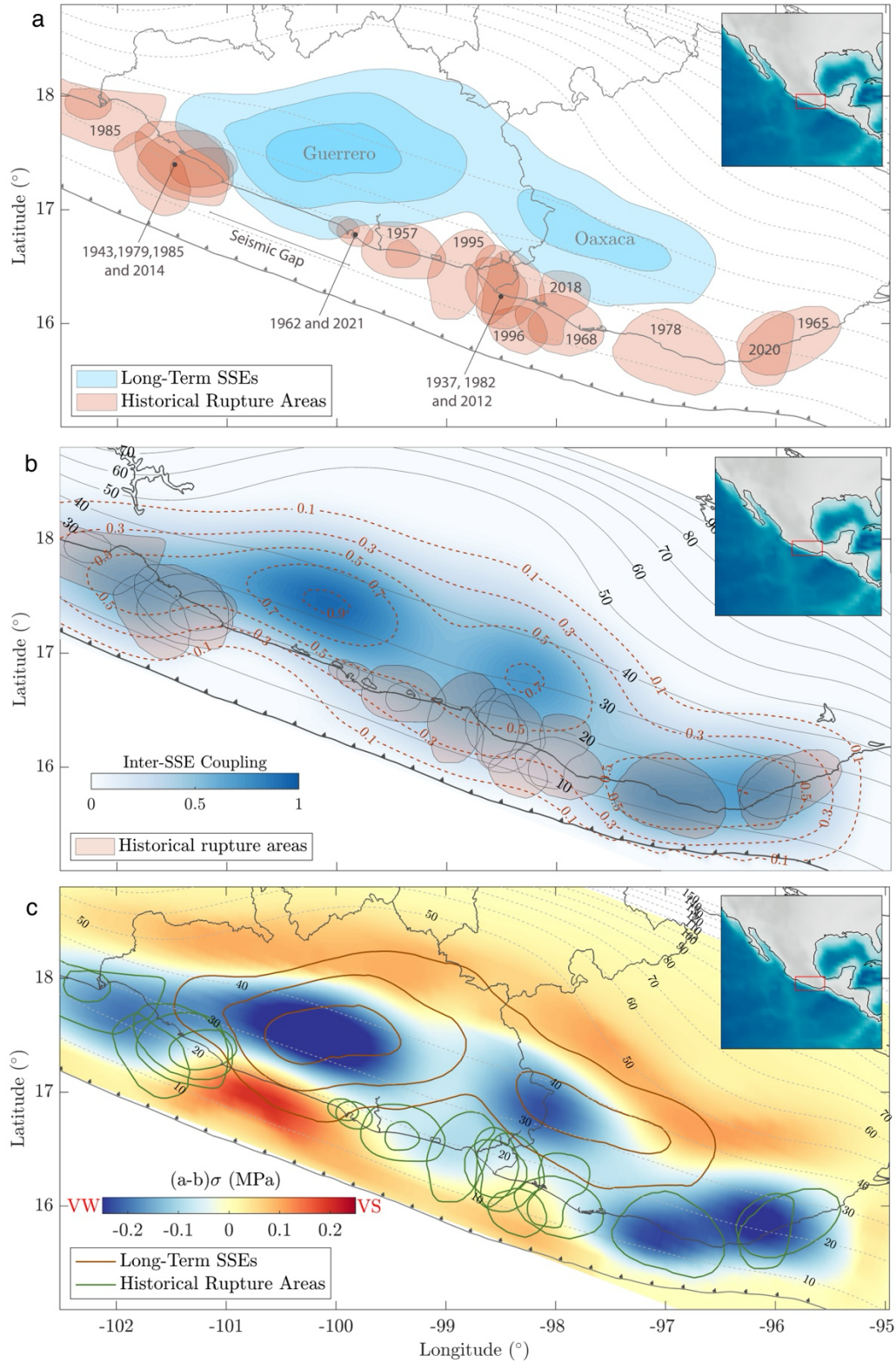


**Figure 5** (a) Average slip distribution of all inverted SSEs (blue shades; see Figure 1) (Cruz-Atienza et al., 2025a) together with the rupture areas of large earthquakes (red shades). (b) Interplate coupling distribution determined from inter-SSE periods (see Figure S2). (c) Distribution of the dynamic condition  $(a-b)\sigma_{ss}$  over the plate interface derived from deformation data during steady-state inter-SSE periods (see Figure S6).

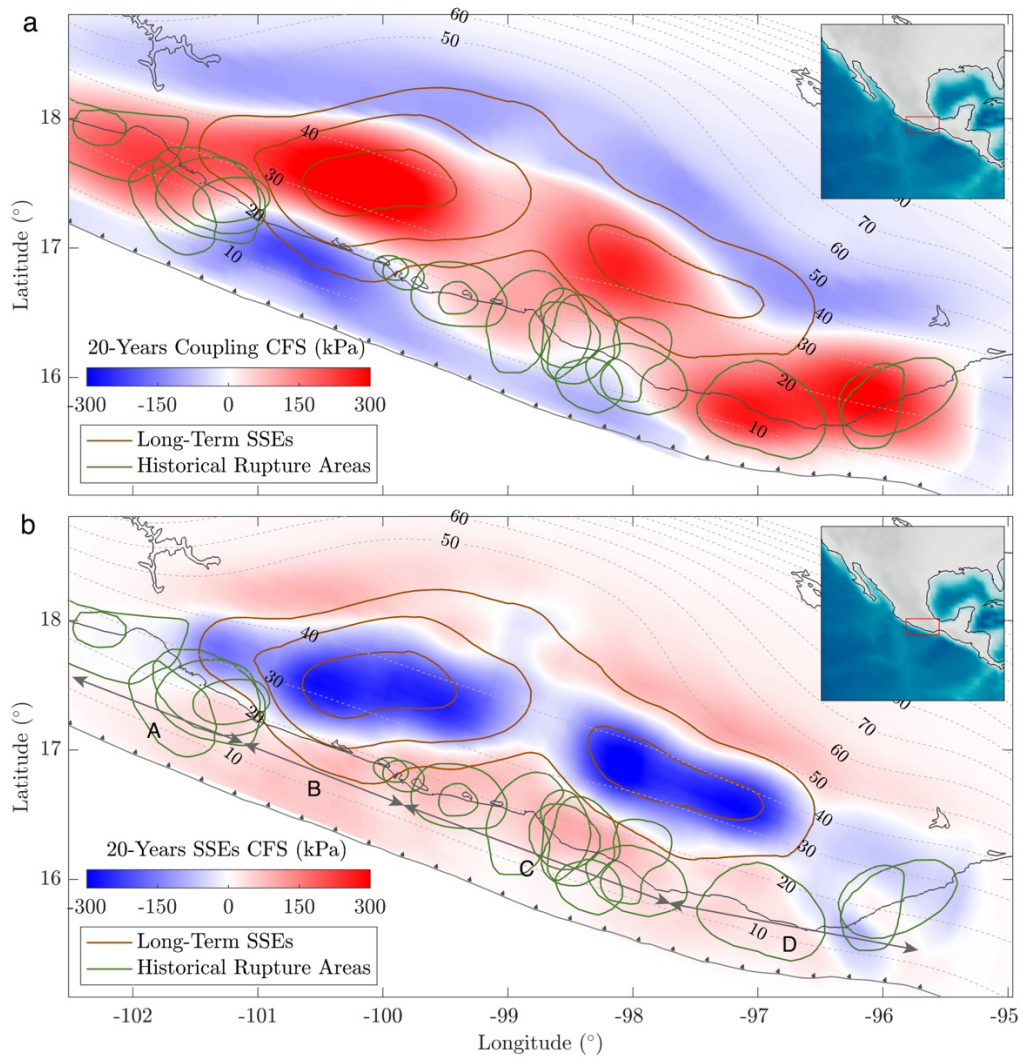


**Figure 6** Cumulative Coulomb failure stress (CFS) over 20 years (i.e., between 2002 and 2022) associated (a) with interplate coupling and (b) with the 25 known SSEs in the region (see Figure 1) (Cruz-Atienza et al., 2025a). As a reference, the brown contours indicate the average SSE iso-slip values shown in Figure 5a.



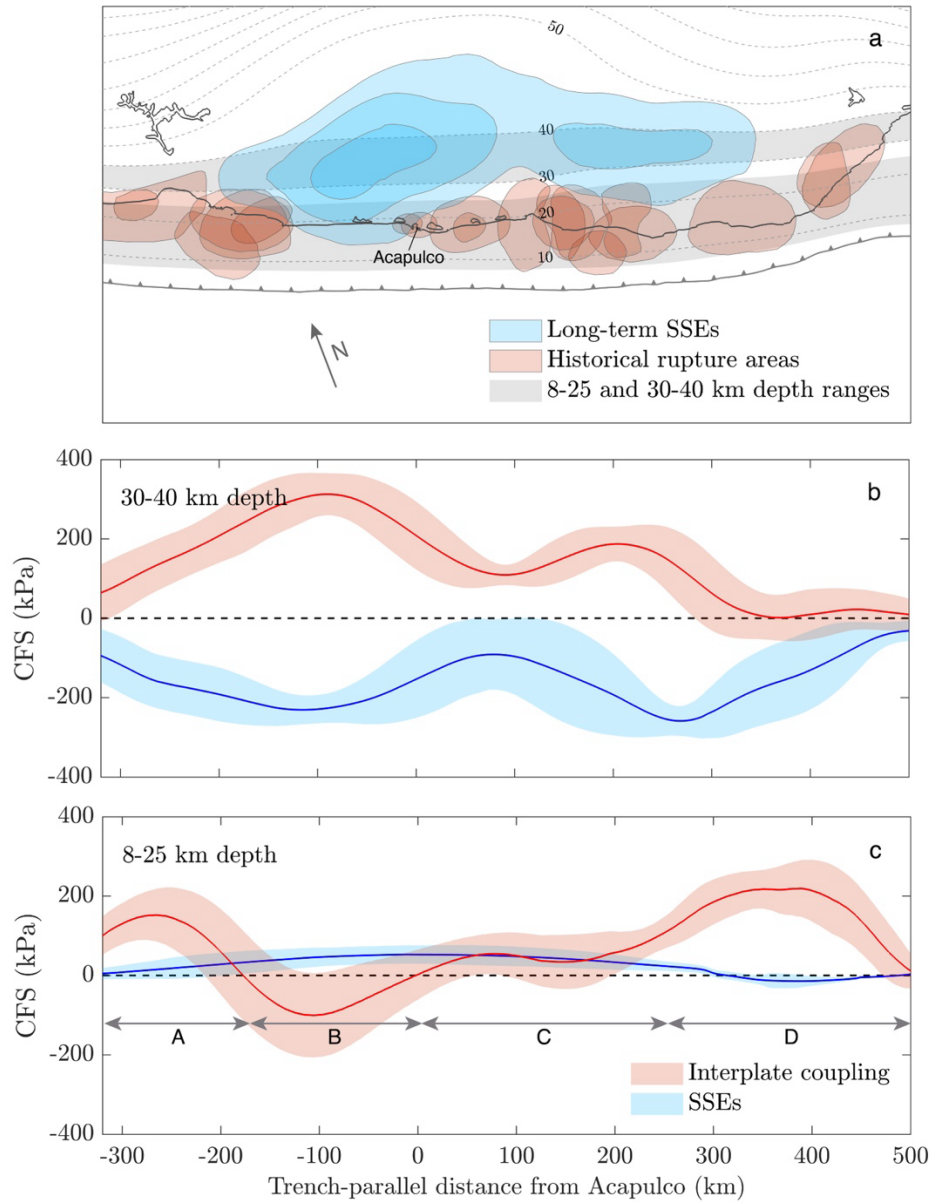


**Figure 7** Distribution of cumulative Coulomb failure stress (CFS) over 20 years (i.e., between 2002 and 2022) at the plate interface due to coupling and SSEs along the trench-parallel direction from Acapulco, averaged in depth ranges of (b) 30-40 km and (c) 8-25 km (gray shades in panel a). Segments A, B, C and D in panel c are also indicated in Figure 6b.

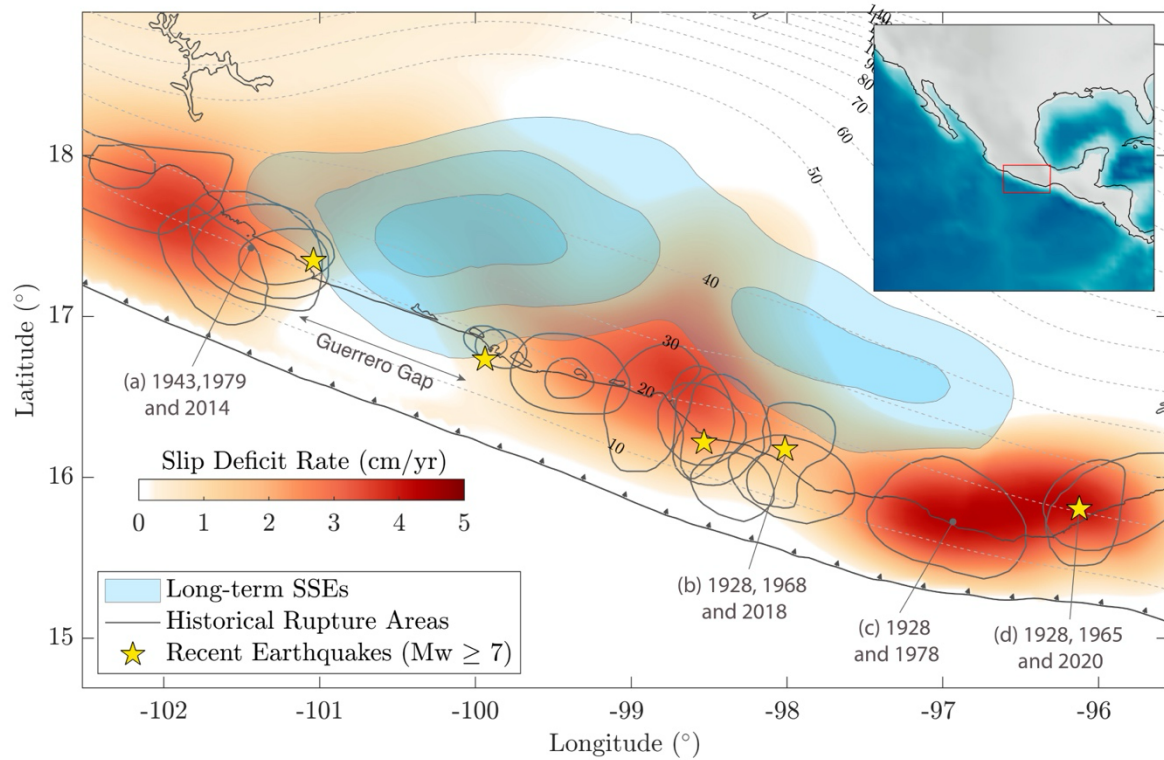


**Figure 8** Slip deficit rate at the plate interface derived from the regional plate convergence and the cumulative aseismic slip over 20 years due to coupling and SSEs (see Figure S7). Sequences of large (M7+) repeating earthquakes (a-d) are indicated after Singh et al. (2024). Sequence (a) is not repeating but the magnitudes and rupture areas of successive earthquakes are similar.

	Earthquake sequence	Average slip	Slip deficit prediction
(a)	1943, 1979, 2014 (M7.3)	1.71 m	$1.24 \pm 0.03$ m
(b)	1928, 1968, 2018 (M7.2)	1.53 m	$1.18 \pm 0.18$ m
(c)	1928, 1978 (M7.6)	2.42 m	2.25 m
(d)	1928, 1965, 2020 (M7.4)	1.93 m	$1.99 \pm 0.55$ m

**Table 1** Estimates of the average slip ( $\bar{d}$ ) for the sequences of M7+ repeating earthquakes (a-d in Figure 8) found by Singh et al. (2024) compared with the slip estimates predicted by the slip deficit rate shown in Figure 8. Sequence (a) is not repeating but successive earthquakes are similar.